

Truncated Conformal Space Approach for Perturbed Wess-Zumino-Witten $SU(2)_k$ Models

M. Beria,¹ G. P. Brandino,² Luca Lepori,^{3,4} R. M. Konik,⁵ and G. Sierra⁶

¹*SISSA-International School for Advanced Studies,
Via Bonomea 265, I-34136 Trieste,
Italy EU, and INFN, Sezione di Trieste.*

²*Institute for Theoretical Physics, University of Amsterdam,
Science Park 904, Postbus 94485, 1090 GL Amsterdam, The Netherlands.*

³*Departament de Física, Universitat Autònoma de Barcelona, E-08193 Bellaterra, Spain.*

⁴*IPCMS (UMR 7504) and ISIS (UMR 7006),
Université de Strasbourg and CNRS, Strasbourg, France.*

⁵*Condensed Matter and Material Science Department,
Brookhaven National Laboratory, Upton NY 11973-5000, USA.*

⁶*Instituto de Física Teórica, UAM-CSIC, Madrid, Spain.*

Abstract

We outline the application of the truncated conformal space approach (TCSA) to perturbations of $SU(2)_k$ Wess-Zumino-Witten theories. As examples of this methodology, we consider two distinct perturbations of $SU(2)_1$ and one of $SU(2)_2$. $SU(2)_1$ is first perturbed by its spin-1/2 field, a model which is equivalent to the sine-Gordon model at a particular value of its coupling β . The sine-Gordon spectrum is correctly reproduced as well as the corresponding finite size corrections. We next study $SU(2)_1$ with a marginal current-current perturbation. The TCSA results can be matched to perturbation theory within an appropriate treatment of the UV divergences. We find however that these results do not match field theoretic computations on the same model performed with a Lorentz invariant regulator. Finally, we consider $SU(2)_2$ perturbed by its spin-1 field, which is equivalent to three decoupled massive Majorana fermions. In this case as well the TCSA reproduces accurately the known spectrum.

I. INTRODUCTION

Correlations in one dimensional systems typically require non-perturbative, non-mean field techniques to access the underlying physics. These techniques often trade on low energy, field theoretical reductions of the system. Examples include bosonization [1], conformal field theory [2], integrable field theory [3], the Bethe ansatz [4], and the truncated conformal spectrum approach (TCSA) [5]. The last approach, unlike the aforementioned techniques, is able to deal in principle with any one dimensional field theory in an exact numerical manner. In that sense the TCSA is similar to the density matrix renormalization group (DMRG) [6], but the framework where it is formulated is field theoretical and not discrete quantum lattice systems.

TCSA deals with models whose Hamiltonians can be represented in the form,

$$H = H_{CFT} + \Phi, \tag{1}$$

where H_{CFT} is the Hamiltonian of some conformal field theory and Φ is an arbitrary perturbation. The approach employs the Hilbert space of the conformal field theory as a computational basis and exploits the ability to compute matrix elements of the perturbing field in this same basis using the constraints afforded by the conformal symmetry. It was first employed by Yurov and Zamolodchikov in studies of massive perturbations of the critical Ising model [7] and the scaling Yang-Lee model [5].

Since its introduction it has been used in a large number of instances and to some degree has become a standard tool. It has been used to study perturbations of the tri-critical Ising [8, 9], the 3-states Potts model [10], bosonic ($c = 1$) compactified theories [11], the sine-Gordon model [12, 13], and perturbations of boundary conformal field theories [14]. Spectral flows between different conformal field theories were addressed in Ref. [15], while the correctness of the thermodynamic Bethe ansatz equations was checked in Refs. [16, 17]. Finite-size corrections to the mass spectra have also been analyzed in Refs. [18, 19]. By replacing the conformal field theory with an integrable field theory, the approach can also study models of perturbed integrable field theories. Matrix elements of the perturbing field are then computed in the form factor bootstrap approach [20].

While the TCSA approach is extremely flexible in the models it can attack, it is in practice limited to perturbations of conformal field theories with small central charge ($c \lesssim 1$).

For theories with large central charge, the underlying conformal Hilbert space is large and becomes numerically burdensome to manipulate. The difficulty has recently been partially ameliorated with the development of a numerical renormalization group (NRG) for the TCSA [21–25]. This renormalization group permits large Hilbert spaces to be dealt with piecewise making the numerics manageable. Using this renormalization group, the excitonic spectrum of semi-conducting carbon nanotubes was studied [24] (here the underlying conformal field theory had $c = 4$) as were large arrays of coupled quantum Ising chains [22] (here the underlying conformal field theory had $c \sim 30 - 50$).

The TCSA approach, as designed, focuses on accurately computing the properties of the low energy states. However when combined with an NRG together with a sweeping algorithm not dissimilar to the finite volume algorithm of the DMRG [6], the TCSA can compute the properties of states over a wide range of energies. This was demonstrated in [23] where the level spacing statistics were studied in crossing over from an integrable to a non-integrable model.

To the best of our knowledge the TCSA has not been applied previously to perturbations of Wess-Zumino-Witten (WZW) models. WZW models are non-linear sigma models whose field g lives on a group manifold G . They possess topological terms, the Wess-Zumino term, whose action is quantized with the consequence that its coupling constant k is constrained to be a positive integer. The consequence of the topological term is to make the sigma models conformal with the affine Lie algebra associated with G , spectrum generating. Affine Lie algebras typically have richer structure than the Virasoro algebra and are consequently more difficult to treat with the TCSA. Specialized code needs to be developed in order to treat such models. Here we report the development of such code for the study of perturbations of $SU(2)_k$ WZW models.

Perturbed $SU(2)_k$ WZW models are interesting physically primarily because they are able to represent the low energy structure of spin chains [26]. The most important example here is the spin-1/2 Heisenberg chain, whose low energy behavior is governed by $SU(2)_1$ perturbed by a marginally irrelevant current-current interaction. Adding different perturbations to $SU(2)_1$ leads to different variants of the Heisenberg model. The Hamiltonian

$$H = H_{SU(2)_1} + g \int dx \bar{J}_R \cdot \bar{J}_L + h \int dx (\phi_{1/2,1/2} \bar{\phi}_{1/2,-1/2} - \phi_{1/2,-1/2} \bar{\phi}_{1/2,1/2}), \quad (2)$$

where $\phi_{1/2,\pm 1/2}$ are the spin-1/2 fields in $SU(2)_1$, is the low energy reduction of the dimerized

$J_1 - J_2$ Heisenberg model

$$H = \sum_n J_1 (1 + \delta(-1)^n) \bar{S}_n \cdot \bar{S}_{n+1} + J_2 \bar{S}_n \bar{S}_{n+1}. \quad (3)$$

The couplings of the two models are related via $g \propto J_2 - J_{2c}$ and $h \propto \delta$. This model has been studied intensely both field theoretically with RG analyses [27] and with DMRG [28, 29]. These methodologies do not currently agree on how the spin gap depends upon the dimerization parameter δ . It is one of the aims of our work to set up the framework under which disputed questions surrounding this model can be addressed.

$SU(2)_k$ for $k > 1$ WZW theories are also of considerable interest as they are the low energy reductions of families of spin- $k/2$ spin chains with finely tuned, local interactions [26]. They have also been shown more recently to represent Haldane-Shastry type spin chains [30] with longer range interactions [31–33]. In both cases, it is of interest to understand how $SU(2)_k$ WZW behaves in the presence of relevant and marginal perturbations. And more generally, because $SU(2)_k$ WZW theories are multicritical with many possible relevant perturbations. Actual spin chains are likely to be realized only in the vicinity of these critical points rather than precisely at them.

The outline of this paper is as follows. In Section II we present briefly the framework for the TCSA where perturbations of $SU(2)_k$ can be studied. In the next three sections we present applications of the TCSA to perturbed $SU(2)_k$ models, establishing how the methodology works. In Section III we examine the $SU(2)_1 + Tr(g)$ model, which is equivalent to the sine-Gordon model. This allows us to compare our numerics with known analytic results. In Section IV we study the $SU(2)_1 + \bar{J}_L \cdot \bar{J}_R$ model, which corresponds to a marginal current-current perturbation of $SU(2)_1$. We show here that one can isolate the UV divergent behavior, essential for extracting the universal behavior of spin chains described by $SU(2)_k$ with a marginal perturbation. Finally, in Section V, we consider $SU(2)_2$ perturbed by $Tr(g)^2$. This provides a useful benchmark of our methodology as the theory is equivalent to three non-interacting massive Majorana fermions. We close in Section VI with conclusions and a discussion of future directions.

II. TCSA FOR $SU(2)_k$ WZW MODELS

In this section we describe the application of the TCSA [5] to deformations of the $SU(2)_k$ Wess-Zumino-Witten model [34, 35]. We thus start by considering Hamiltonians of the form

$$H = H_{SU(2)_k} + g \int_0^R dx \Phi(x). \quad (4)$$

Here Φ is a spin singlet combination of (highest weight or current) fields of the WZW model. The Hamiltonian is defined on a circle of length R . Adding the time coordinate the underlying space-time is an infinite cylinder with circumference R .

The first step in the TCSA is to characterize the unperturbed theory, $H_{SU(2)_k}$. This theory provides the computational basis of the TCSA numerics. $H_{SU(2)_k}$ has central charge $c = 3k/(k+2)$ ($k = 1, 2, \dots$), and can be written à la Sugawara in terms of the $SU(2)_k$ currents:

$$\begin{aligned} H_{SU(2)_k} &= \frac{2\pi}{R} \left(L_0 + \bar{L}_0 - \frac{c}{12} \right) \\ &= \frac{2\pi}{R} \left(\sum_m : \left[(2J_m^0 J_{-m}^0 + J_m^+ J_{-m}^- + J_m^- J_{-m}^+) \right. \right. \\ &\quad \left. \left. + (2\bar{J}_m^0 \bar{J}_{-m}^0 + \bar{J}_m^+ \bar{J}_{-m}^- + \bar{J}_m^- \bar{J}_{-m}^+) \right] : - \frac{c}{12} \right). \end{aligned} \quad (5)$$

The left-moving currents $J_m^{0,\pm}$ obey the algebra,

$$\begin{aligned} [J_m^0, J_n^0] &= \frac{km}{2} \delta_{n+m,0}, \\ [J_m^0, J_n^\pm] &= \pm J_{m+n}^\pm, \\ [J_m^+, J_n^-] &= 2J_{m+n}^0 + km \delta_{m+n,0}, \end{aligned} \quad (6)$$

with the right moving currents $\bar{J}_m^{0,\pm}$ obeying the same algebra.

The field content of $H_{SU(2)_k}$ consists of $k+1$ primary fields, $\phi_{s,m=-s,\dots,s}$, forming spin $s = 0, \dots, k/2$ representations. The conformal weight of the spin s primary field is given by $\Delta_s = s(s+1)/(k+2)$. The primary fields and the WZW currents are the basic tools to construct the Hilbert space of the unperturbed theory, providing the first ingredient of the TCSA. The Hilbert space can be written as a tensor product of its holomorphic (left) and anti-holomorphic (right) degrees of freedom. For $SU(2)_k$, the left and right sectors of the Hilbert space each have $k+1$ modules, where each module is associated to one primary

field. The module consists of a highest weight state, $|s, s\rangle \equiv \phi_{s,s}(0)|0\rangle$, together with an infinite tower of descendant states:

$$J_{-n_M}^{a_M} \dots J_{-n_1}^{a_1} |\phi_{s,s}\rangle, \quad n_i = 0, 1, 2, \dots \quad a_i = 0, \pm. \quad (7)$$

These states (7) are eigenstates of the Virasoro operator L_0 ,

and the third component component of the current J_0^0 :

$$L_0 (J_{-n_M}^{a_M} \dots J_{-n_1}^{a_1}) |s, s\rangle = \left[\Delta_s + \sum_i n_i \right] (J_{-n_M}^{a_M} \dots J_{-n_1}^{a_1}) |s, s\rangle; \quad (8)$$

$$J_0^0 (J_{-n_M}^{a_M} \dots J_{-n_1}^{a_1}) |s, s\rangle = \left[s + \sum_i a_i \right] (J_{-n_M}^{a_M} \dots J_{-n_1}^{a_1}) |s, s\rangle.$$

The quantity $\sum_i n_i$ is called the Kac-Moody level, or simply the level, of the descendant state.

The set of states (7) is not yet a basis of the Hilbert space since it is over complete and contains null states. In order to form a complete orthonormal basis, we tackle each Kac-Moody module separately.

We do so in an iterative fashion. At each step we have a set of non-zero norm states which are linearly independent (at the beginning this set will consist solely of the highest weight state). We next add a new descendant state to this set, compute the matrix of scalar products of states in the expanded set (the Gramm matrix), and find its determinant. If it is non-zero, the new state is added to the list; otherwise it is discarded. We then move to the next descendant in the tower of states in increasing order in the level. The process ends when all the states up to a given level have been considered.

This procedure yields a complete set of states that we can easily orthonormalize to obtain a basis. In order to optimize this procedure we take into account the following properties:

- states with different L_0 quantum number are independent;
- states having different spin (eigenvalue of J_0^0) are independent;
- we discard the states with null norm;
- we act only with level 0 currents, $J_0^{0,\pm}$, directly on the highest weight state $|s, s\rangle$ in the module.

	$SU(2)_1$		$SU(2)_2$		
level	I	1/2	I	1/2	1
0	1	2	1	2	3
1	4	4	4	8	7
2	8	10	13	20	19
3	15	18	28	46	40
4	28	32	58	94	83
5	47	52	112	178	152
6	76	86	206	324	275
7	119	132	359	564	468
8	181	202	611	948	786
9	271	298	1002	1552	1272
10	397	436	1611	2482	2026
11	571	622	2529	3886	3145

TABLE I: The dimensions of the Verma modules of $SU(2)_1$ and $SU(2)_2$ at different levels.

To demonstrate that the above method amounts to a numerically intensive task, we present in Table I the number of states per level for the two modules of $SU(2)_1$ and the three modules of $SU(2)_2$.

Once the chiral sector of $SU(2)_k$ has been obtained, the total Hilbert space is constructed as a tensor product of the isomorphic holomorphic and antiholomorphic sectors. These tensor products are diagonal in the modules, i.e. left moving spin s states are only tensored with their right moving spin s counterparts. In forming these tensor products, we group the states by their value of Lorentz spin, $(L_0 - \bar{L}_0)$, and z -component of $SU(2)$ spin, $J_0^0 + \bar{J}_0^0$. Recall that the Lorentz spin is proportional to the momentum carried by the corresponding state. In Table II we present the number of cumulative states up to a given level in $SU(2)_1$ and $SU(2)_2$ with vanishing Lorentz spin.

Once the computational basis has been constructed, the TCSA requires the evaluation of matrix elements of the perturbing operator in that basis. For this purpose one uses the commutation relations of the fields, $\phi_{s,m}(0)$, with the current modes, $J_0^{0,\pm}$, which are given

$SU(2)_1$ level	mom. 0	$SU(2)$ spin 0	$SU(2)_2$ level	mom. 0	$SU(2)$ spin 0
1	18	8	1	75	25
2	70	24	2	444	120
5	1309	381	4	6839	1595
11	133123	32021	7	185111	38665

TABLE II: The cumulative dimensions for non chiral spaces at given level with total Lorentz spin (mom.) zero (first column) and both Lorentz spin and $SU(2)$ spin S_z zero (second column).

$SU(2)_1$			
$C_{0,0;1/2,-1/2;1/2,1/2}$	1	$C_{1/2,1/2;1/2,1/2;0,0}$	1
$SU(2)_2$			
$C_{0,0;1/2,-1/2;1/2,1/2}$	1	$C_{1,1;1,1;0,0}$	1
$C_{0,0;1,-1;1,1}$	1	$C_{1,1;1/2,1/2;1/2,1/2}$	1
$C_{1/2,1/2;1/2,1/2;0,0}$	1	$C_{1/2,1/2;1/2,-1/2;1,1}$	-1
$C_{1/2,1/2;1,0;1/2,1/2}$	$-\frac{1}{\sqrt{2}}$		

TABLE III: Non zero structure constants of $SU(2)_1$ and $SU(2)_2$.

by

$$\begin{aligned}
[J_0^0, \phi_{s,m}] &= m \phi_{s,m}; \\
[J_0^\pm, \phi_{s,m}] &= (s \pm m) \phi_{s,m\pm 1}.
\end{aligned} \tag{9}$$

With these commutation relations and those of the current modes (6), matrix elements of the form

$$\langle \phi_{s,s} | J_{n_1}^{a_1} \cdots J_{n_m}^{a_m} \phi_{s',m}(0,0) J_{-l_1}^{b_1} \cdots J_{-l_k}^{b_k} | \phi_{s'',s''} \rangle, \tag{10}$$

can be reduced to the structure constants, $C_{s_1,m_1;;s_2,m_2;s_3,m_3}$:

$$\langle \phi_{s,s} | \phi_{s'm}(0) | \phi_{s'',s''} \rangle = \left(\frac{2\pi}{R} \right)^{2\Delta_s} C_{s,s;s',m;s'',s''}. \tag{11}$$

We list all non-zero structure constants, $C_{s_1,m_1;;s_2,m_2;s_3,m_3}$ in Table III for $SU(2)_1$ and $SU(2)_2$.

With the spectrum of the unperturbed $SU(2)_k$ model specified and the matrix elements of the perturbing field given, we are able to compute explicitly the matrix elements of the full Hamiltonian on the circle and represent it in matrix form. To be able to analyze this

Hamiltonian, we truncate (the truncation in the acronym TCSA) the Hilbert space by discarding all states with a chiral component whose level is greater than N_{tr} . The resulting *finite* dimensional Hamiltonian matrix can then be diagonalized numerically, obtaining the spectrum of the perturbed theory. This procedure is particularly robust for relevant perturbations since the low energy eigenstates of the perturbed theory, $|r\rangle$, are localized on the low energy conformal states, $\{|c\rangle_\alpha\}$. Namely, expanding $|r\rangle$ into the conformal basis, $\{|c\rangle_\alpha\}$,

$$|r\rangle = \sum_{\alpha} b_{\alpha} |c\rangle_{\alpha}, \quad (12)$$

the coefficients b_{α} , are primarily concentrated on the low energy conformal states $|c\rangle_{\alpha}$ determined by $H_{SU(2)_k}$.

To extract physical quantities for the perturbed Hamiltonian (4), such as the mass gap, energy levels, correlation functions, etc., the choice of the system size, R , requires special consideration. For $mR \ll 1$ (here m is the putative mass scale of the perturbed theory), the system lies in the UV limit where the conformal term, $H_{SU(2)_k}$, of the full Hamiltonian dominates. In this regime the spectrum resembles that of the conformal $H_{SU(2)_k}$ where the energy levels scales as $1/R$. In the IR regime, $Rm \gg 1$, the perturbation, $\int dx \Phi(x)$, dominates and one expects a scaling of the form $\sim R^{1-2\Delta_s}$, where $2\Delta_s$ is the scaling dimension of the perturbing field. In general, the spectrum of the perturbed model must be extracted in a region of R where the conformal term and the perturbation are balanced in the sense that physical quantities remains stable under small variations of R . This region is usually denoted as the ‘‘physical window’’.

For theories where the dimension of the Hilbert space grows very fast, i.e. $SU(2)_k$ with k large, the truncation scheme proposed above may not yield accurate results.

In those cases one can take recourse to a numerical renormalization group (NRG) improvement of the TCSA [21–25]. This procedure allows the TCSA to reach much higher truncation levels than that possible in its unadorned form. Taken together with an analytic renormalization group, it is possible to remove the effects of truncation altogether [21]. While this NRG has been tested extensively on relevant perturbations of conformal field theories, it has not hitherto been tried on marginal perturbations of CFTs. We will show in Section IV that the NRG can accurately predict the low lying spectrum even in the marginal case.

III. $SU(2)_1$ PERTURBED BY THE SPIN-1/2 FIELD

Our first test of the TCSA is the perturbation of the $SU(2)_1$ WZW model by the singlet formed from the spin-1/2 operator of $SU(2)_1$, $\Phi = (\phi_{1/2,1/2} \bar{\phi}_{1/2,-1/2} - \phi_{1/2,-1/2} \bar{\phi}_{1/2,1/2})$:

$$H_{rel} = H_{SU(2)_1} + h \int dx \Phi(x). \quad (13)$$

The scaling dimension of Φ is $2\Delta_{1/2} = 1/2$, and so this is a relevant perturbation. Moreover the theory is invariant under $h \rightarrow -h$. This Hamiltonian is equivalent to the sine-Gordon model whose Lagrangian is given by [36]

$$L_{SG} = \int d^2x \left(\frac{1}{2} (\partial_\mu \varphi)^2 + 2\lambda \cos(\beta\varphi) \right), \quad (14)$$

with $\beta^2 = 2\pi$. The correspondence between (13) and (14) is based on the identifications

$$\phi_{1/2,1/2}(z) = \exp\left(i\frac{\varphi(z)}{\sqrt{2}}\right); \quad \phi_{1/2,-1/2}(z) = \exp\left(-i\frac{\varphi(z)}{\sqrt{2}}\right), \quad (15)$$

which, up to phase redefinitions, are the bosonization formulas of the $SU(2)_1$ model [2].

We now demonstrate that the TCSA numerics reproduce the expected behavior of the sine-Gordon model at this value of the SG coupling. The spectrum of the sine-Gordon model at $\beta^2 = 2\pi$ is composed of a soliton S and antisoliton \bar{S} with mass M and two breathers B_1 and B_2 with masses $M_1 = M$ and $M_2 = \sqrt{3}M$ respectively. The soliton, anti-soliton, and the first breather form a triplet under $SU(2)$. The charges of the particles (S, B_1, \bar{S}) are given by $(1,0,-1)$ and they coincide with their S_z quantum number. The second breather, B_2 , is a singlet under $SU(2)$.

Fig. 1 shows the low energy TCSA spectrum which reproduces the basic structure: a low lying triplet with mass M , and a single excitation at roughly $\sqrt{3}M$. The expected value of the mass M can be determined from the coupling constant used in the TCSA. The relation between the coupling of the sine-Gordon model and the mass M is given as [37]

$$h = \lambda = \frac{\Gamma(\frac{\beta^2}{8\pi})}{\pi\Gamma(1 - \frac{\beta^2}{8\pi})} \left[M\sqrt{\pi} \frac{\Gamma(\frac{1}{2} + \frac{\xi}{2\pi})}{2\Gamma(\frac{\xi}{2\pi})} \right]^{2 - \frac{\beta^2}{4\pi}}, \quad (16)$$

where $\xi = \frac{\beta^2}{8} \frac{1}{1 - \frac{\beta^2}{8\pi}} = \frac{\pi}{3}$. With $h = 0.0942753..$ we expect the mass to be 1 while from the TCSA we find $M = 1.0016$, in excellent agreement.

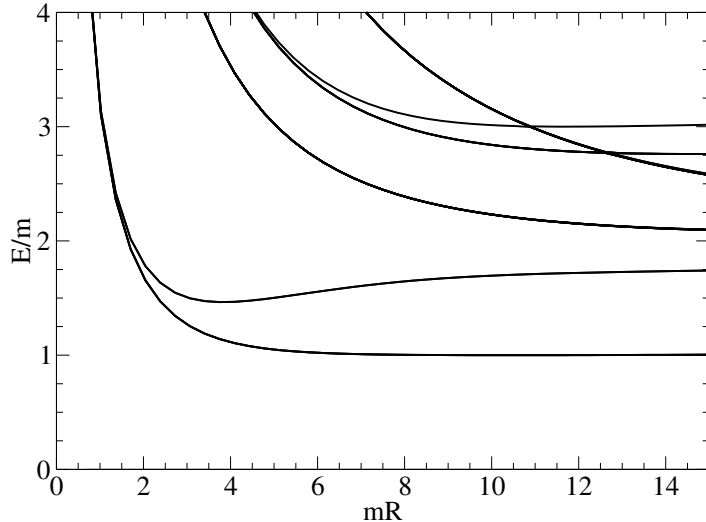


FIG. 1: Plot of the TCSA data for the lowest six excited states in the $S_z = 0$ sector with the ground state energy subtracted. The lowest two excited states correspond to B_1 (the $S_z = 0$ state of the triplet) and B_2 . The next four excited states are two particle states. The data are computed with a truncation level $N_{tr} = 9$. The fundamental triplet of particles can be seen to have mass $M=1.0016$.

For the second breather, found roughly at $\sqrt{3}M$, a more careful analysis of the TCSA data is required. For this excitation there are significant finite size corrections. These corrections can be understood as virtual processes on the cylinder [5, 18], which are suppressed exponentially as R becomes large. For B_2 these corrections are given by [18]

$$\Delta m_{B_2}(R) = -3\sqrt{3}e^{-R/2} - \int_{-\infty}^{\infty} \frac{d\theta}{2\pi} e^{-m_{B_2}R \cosh\theta} m_{B_2}R \cosh(\theta) (S_{B_2B_2}^{B_2B_2}(\theta + i\pi/2) - 1) + \mathcal{O}(e^{-\sigma_{B_2}R}). \quad (17)$$

We can estimate the so-called error exponent to be $\sigma_{B_2} = 1.105$ [18]. Here $S_{B_2B_2}^{B_2B_2}(\theta)$ is the scattering S -matrix of the process $B_2 + B_2 \rightarrow B_2 + B_2$ [38]. Fitting $m_{B_2} + \Delta m_{B_2}(R)$ to the TCSA data, we find that $M_{B_2}/M = 1.7322 \pm 0.0003$. Using this mass, we plot $m_{B_2} + \Delta m_{B_2}$ against the TCSA data in Fig. 2, which shows an excellent agreement between the theory and the TCSA data for $R > 9$.

We now turn to the ground state energy E_{gs} . The TCSA gives E_{gs} as would be computed in conformal perturbation theory to all orders. This perturbative energy can be expressed as the sum of a linear term in R , proportional to a bulk energy density, ϵ_{bulk} , plus a term

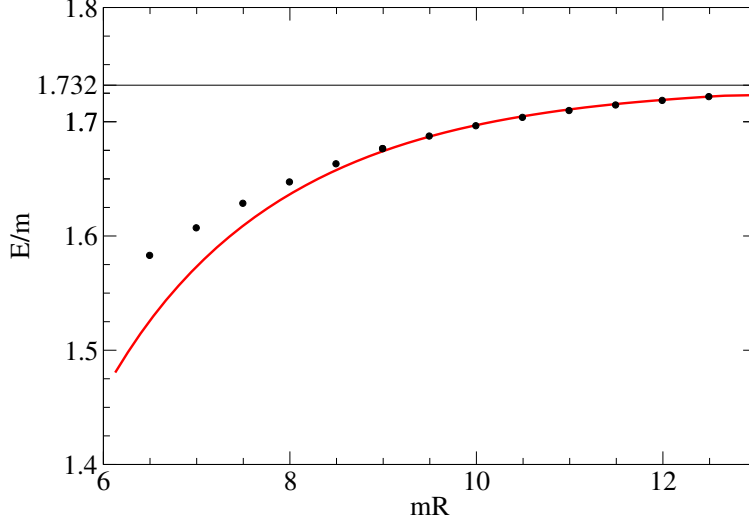


FIG. 2: Single particle state B_2 : Analytic prediction for its mass with finite size effects (continuous line) compared to the TCSA data.

given by the thermodynamic Bethe ansatz E_{TBA} [5, 39].

$$E_{gs} = \epsilon_{\text{bulk}}R + E_{TBA}(R). \quad (18)$$

The bulk contribution to E_{gs} is given by [40]

$$\epsilon_{\text{bulk}} = -\frac{M^2}{4} \tan \frac{\xi}{2} = -\alpha M^2 R. \quad (19)$$

For sine-Gordon with $\beta^2 = 2\pi$, $\alpha = 0.14438\dots$. The contribution from $E_{TBA}(R)$ is given by the solution of a coupled set of integral equations involving the S -matrices of the various excitations in the model [5, 39]. At large R , this contribution reads

$$E_{TBA}(R) = -3M \int_{-\infty}^{\infty} \frac{d\theta}{2\pi} \cosh(\theta) e^{-MR \cosh(\theta)} - \sqrt{3}M \int_{-\infty}^{\infty} \frac{d\theta}{2\pi} \cosh(\theta) e^{-\sqrt{3}MR \cosh(\theta)} + \mathcal{O}(e^{-2MR}), \quad (20)$$

and essentially marks the correction to the energy due to the spontaneous emission of a virtual particle from the vacuum which travels around the system before being reabsorbed. Fig. 3 shows the TCSA data against the theoretical values of E_{gs} (including the full, not just the leading order large R , contribution coming from $E_{TBA}(R)$). There is a good agreement for R smaller than $mR = 8$ and then slight deviations thereafter, which can be reduced by increasing the value of N_{tr} (see Fig. 3).

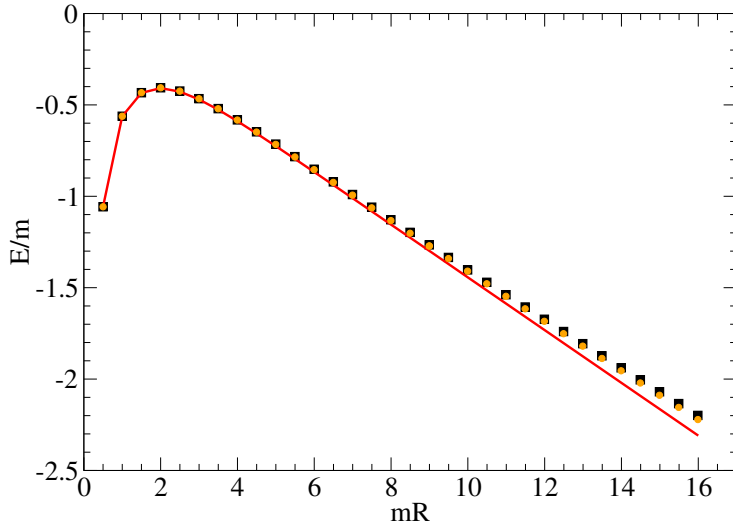


FIG. 3: Ground state energy: analytic prediction (continuous line) compared to the TCSA results. Black squares: TCSA with $N_{tr} = 9$; orange circles: TCSA with $N_{tr} = 10$.

Above the single particle states, one encounters sets of two-particle states consisting of pairs of particles from the triplet and the singlet of the SG model. These two-particle states can be organized into $SU(2)$ multiplets. For example, two-particle states involving the triplet decompose as $(\mathbf{3} \otimes \mathbf{3}) = (\mathbf{5} \oplus \mathbf{3} \oplus \mathbf{1})$. These states suffer finite size corrections due to scattering between the particles. These effects can be taken into account by solving the quantization conditions for the momentum in finite volume:

$$2\pi n_i = mR \sinh \theta_i - i \ln S_{ij}(\theta_i - \theta_j), \quad i = 1, 2, \quad (21)$$

where θ_i ($i = 1, 2$) are the rapidities of the particles that parametrize their energy-momentum, $(E, p) = (m \cosh \theta_i, m \sinh \theta_i)$, and S_{ij} is the scattering matrix between the two particles [41]. The solution of these equations, for a pair (n_1, n_2) , yields the rapidities as a function of R , and so the energy of these states. Fig. 4 shows reasonably good agreement between the analytical and the TCSA results, particularly at large values of R . At smaller R , single particle virtual processes become important, leading to deviations between the TCSA and our analytic estimates.

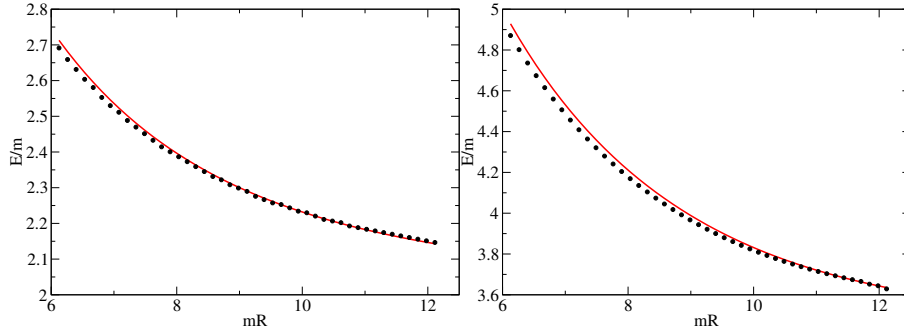


FIG. 4: Two-particle states: comparison between the analytic results and the TCSA data. Left panel: a two particle state involving two triplet particles with total $S_z = 0$ and $(n_1, n_2) = (-1, 1)$. Right panel: a two-breather B_2 state with $(n_1, n_2) = (-1, 1)$. Continuous line: analytical results derived from Eqn. (21). Dots: TCSA data.

IV. $SU(2)_1$ PERTURBED BY CURRENT-CURRENT INTERACTIONS

In this section we consider the perturbation of the $SU(2)_1$ WZW model by the marginal current-current operator,

$$H = H_{SU(2)_1} - g \int dx \bar{J}_L(x) \cdot \bar{J}_R(x). \quad (22)$$

Unlike the perturbation by the spin-1/2 field, here the sign of g matters as it differentiates the model's behavior in the IR limit [38]. For $g > 0$ the perturbation is marginally relevant and asymptotically free. The corresponding theory is a massive integrable rational field theory (RFT) coinciding with the $SU(2)$ Thirring model [42]. And for $g < 0$ the coupling is marginally irrelevant and the theory undergoes a massless RG flow towards the $SU(2)_1$ fixed point.

We address two questions here. We first ask if we can determine with the TCSA the universal correction (as explained below) to the ground state energy due to the marginal perturbation. And second, we question if the numerical renormalization group improvement of the TCSA works in the context of marginal perturbations [21–25].

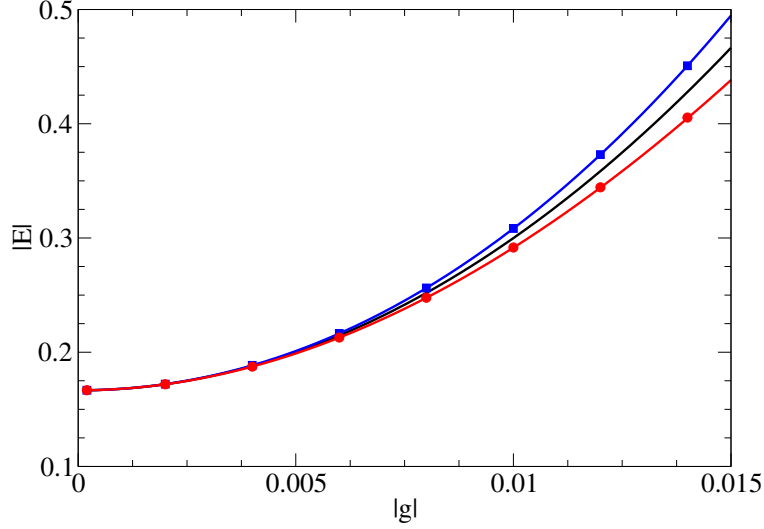


FIG. 5: Plots of the ground state energy of $SU(2)_1 + \bar{J}_L \cdot \bar{J}_R$ as a function of the marginal coupling g . Solid lines give the perturbative computation for both $g > 0$ relevant (blue) and $g < 0$ irrelevant (red). The black line shows the second order perturbative correction in g . The data points represent the corresponding numerical data from the TCSEA.

A. Universal Term in Ground State Energy from the TCSEA

In the small g regime, the correction to the ground state energy on the cylinder is given in perturbation theory by [43]:

$$E_0 = -\frac{\pi}{6R}c - \frac{g^2}{2!}R \left(\frac{2\pi}{R}\right)^{2x-2} \frac{3}{4}I_2 - \frac{g^3}{3!}bR \left(\frac{2\pi}{R}\right)^{3x-4} I_3, \quad (23)$$

where

$$I_2 = \int d^2z |z|^{x-2} |z-1|^{-2x},$$

$$I_3 = \int d^2z_1 d^2z_2 |z_1|^{x-2} |z_2|^{x-2} |z_1-1|^{-x} |z_2-1|^{-x} |z_1-z_2|^{-x}. \quad (24)$$

We write these expressions so that they are valid for a general dimension, x , of the perturbing operator, $\phi(= \bar{J}_L \cdot \bar{J}_R$ for $x = 2$). Our conventions are such that two point function of ϕ is (on the plane)

$$\langle \phi(r)\phi(0) \rangle = \frac{3}{4} \frac{1}{|r|^{2x}},$$

while its corresponding three point function equals

$$\langle \phi(r_1)\phi(r_2)\phi(r_3) \rangle = \frac{b}{|r_{12}|^x |r_{13}|^x |r_{23}|^x}, \quad (25)$$

with $b = 3/2$. The β -function for this theory in these conventions is given by

$$\frac{d\tilde{g}}{dl} = (2 - x)\tilde{g} + \frac{4\pi b}{3\Gamma^2(x/2)}\tilde{g}^2. \quad (26)$$

where \tilde{g} is then the dimensionless coupling and l is a logarithmic length scale. To convert to the conventions of Refs. [43, 44], we need to take $\phi \rightarrow -\sqrt{\frac{4}{3}}\phi$.

Although the theory is defined on a spacetime cylinder, under a conformal transformation the integrals can be written as integrals over the plane, as given above. The integrals I_2 and I_3 are UV divergent and require regulation. The divergent pieces of these integrals contribute to the non-universal piece of E_0 (non-universal because their value depends on the regulation scheme). If ϵ_p is a short distance regulator in the plane (i.e. the difference of two plane integration variables is not permitted to be smaller than ϵ_p), both I_2 and I_3 contain terms proportional to ϵ_p^{-2} (for $x = 2$). Under a conformal transformation, ϵ_p is related to a short distance regulator on the cylinder, ϵ_c , by $\epsilon_p = 2\pi\epsilon_c/R$. Thus the divergent pieces lead non-universal correction of the form

$$E_{0,non-univ} = (a_2g^2 + a_3g^3 + \dots) \frac{R}{\epsilon_c^{2x-2}}, \quad (27)$$

i.e. these corrections scale linearly with the system size.

On the other hand, the universal corrections coming from I_2 and I_3 are independent of the details of the regulator. Such corrections are usually accessed through analytic continuation in the operator dimension x . For sufficiently small x , the resulting perturbative integrals become convergent. For such a range of x , one then introduces a regulator, ϵ_p , and expands in a Taylor series, finding that I_2 and I_3 have the form [43, 44]:

$$\begin{aligned} I_2(x, \epsilon_p) &= c_2 \epsilon_p^{2(2-x)-2} + I_{2,univ.}(x) + \mathcal{O}(\epsilon_p^{6-2x}); \\ I_3(x, \epsilon_p) &= c_3 \epsilon_p^{3(2-x)-2} + I_{3,univ.}(x) + \epsilon_p^{2-x} I_{3,subleading}(x) + \mathcal{O}(\epsilon_p^{6-2x}); \\ I_{3,subleading}(x) &= -6\pi \frac{\epsilon_p^{2-x}}{2-x} I_{2,univ.}(x). \end{aligned} \quad (28)$$

Because everything is convergent, expressions can be developed for $I_{2,univ.}(x)$ and $I_{3,univ.}(x)$ as a function of x . The universal terms' values close to $x = 2$ are then the analytically continued parts of the expansion of I_2 and I_3 that are independent of the UV regulator (the non-universal terms, in contrast, in general either diverge or vanish close to $x = 2$). The relationship between $I_{3,subleading}(x)$ and $I_{2,univ.}(x)$ arises from the OPE, $\phi\phi \sim b\phi$ [44].

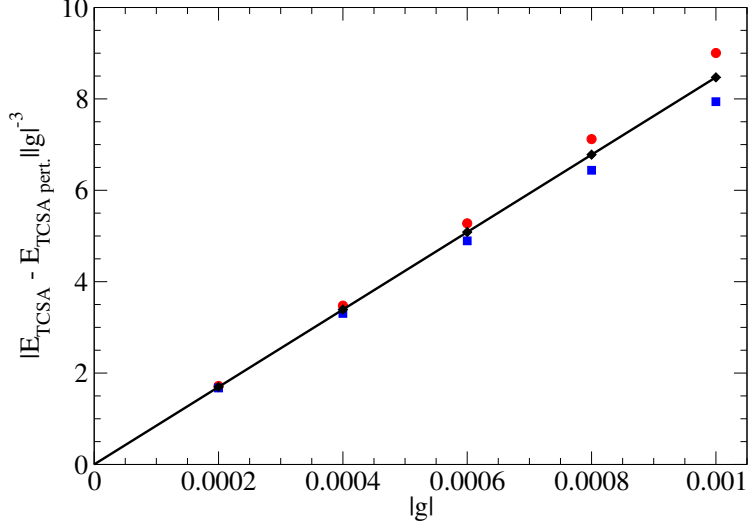


FIG. 6: Plots of the residual ground state energy (the TCSA data with the perturbative contributions, I_2^{TCSA} and I_3^{TCSA} , subtracted off) as a function of g for $N_{tr} = 9$ (red: irrelevant g ; blue: relevant g). The average of the two results (black curve) is fitted with the function, $g^3(a + gbN_{tr}(N_{tr} + 1))$ (this average removes lower order logs that might appear from resumming high order contributions). The fitting parameters are $a = 0.002 \pm 0.001$ and $b = 94.12 \pm 0.02$.

In the case at hand, the universal contributions near $x = 2$ are [43, 44]

$$\begin{aligned}
 I_{2,univ.}(x \sim 2) &= -\frac{\pi}{4}(2 - x); \\
 I_{3,univ.}(x \sim 2) &= -2\pi^2; \\
 I_{3,subleading}(x \sim 2) &= \frac{3\pi^2}{2}.
 \end{aligned} \tag{29}$$

We also include the evaluation of $I_{3,subleading}(x)$ because exactly at $x = 2$ the prefactor of this term becomes independent of ϵ_p . Its evaluation, with important consequences, will turn out to depend upon the choice of regulator.

The universal and subleading parts of I_2 and I_3 allow us to write the universal part of E_0 solely as a function of the running coupling $\tilde{g}(l)$, compatible with scaling theory [44]. $E_{0,univ}$ in terms of the bare dimensionless coupling, $\tilde{g} = g\epsilon_c^{2-x}$, is equal to

$$c(\tilde{g}) \equiv -\frac{6R}{\pi}E_{0,univ} = c + (24\pi) \left(\frac{3}{8}(\epsilon_p^{-y}\tilde{g})^2 I_{2,univ} + \frac{b}{6}(\epsilon_p^{-y}\tilde{g})^3 I_{3,univ} \right). \tag{30}$$

Supposing $y \equiv (2 - x) > 0$, we can use the β -function to express \tilde{g} in terms of $\tilde{g}(l)$:

$$\tilde{g} = \frac{\tilde{g}(l)\epsilon_p^y}{1 - \frac{\tilde{g}(l)}{\tilde{g}^*}(1 - \epsilon_p^y)}, \quad (31)$$

where $\tilde{g}^* = \frac{4\pi b}{3(2-x)} + \mathcal{O}(2-x)$ is the zero of the β -function. We then have

$$c(\tilde{g}(l)) = c + 24\pi \left(-\frac{3}{4} \frac{\pi(2-x)}{8} \tilde{g}^2(l) - \tilde{g}^3(l) \left(\frac{b\pi^2}{12} + \mathcal{O}(2-x) \right) + \mathcal{O}(\tilde{g}^4(l)) \right). \quad (32)$$

$c(\tilde{g}(l))$ is nothing more than Zamolodchikov's c-function [45]. We see that $\partial_{\tilde{g}(l)} c(\tilde{g}(l))$ has the same zero, \tilde{g}^* , as the β -function, as it should. We also see that exactly at the marginal point, $x = 2$, there is a finite third order correction in $\tilde{g}(l)$ to the ground state energy.

An interesting question is what of this universal behavior can be extracted from the TCSA. While it has been suggested in Ref. [15] that the dependency of the TCSA data upon the UV regulator (here, the truncation level, N_{tr}) obscures such terms, it has been shown in Ref. [46] that upon the subtraction of leading and sub-leading order divergences, universal IR behavior can be observed. In answering these questions, the breaking of Lorentz invariance by the TCSA regulator will turn out to be key.

In order to determine the nature of the universal behaviour in the TCSA approach, we need to compute the integrals I_2 and I_3 with the TCSA regulator in place. This however can be straightforwardly done [46]. The essential idea is that these integrals can be expanded in powers of the integration variables $z_{1,2}$. These expansions can then be compared with a Lehmann expansion of the corresponding correlation function (see Appendix A.1). By truncating the Lehmann expansion to the same low energy states used in the TCSA, we are able to compute $I_{2,3}$ with the TCSA regulator. The results precisely at the marginal point $x = 2$ (see Appendices A.2 and A.3 for details) are surprisingly simple and can be computed exactly:

$$\begin{aligned} I_2^{TCSA} &= \pi N_{tr}(N_{tr} + 1); \\ I_3^{TCSA} &= 3\pi^2 N_{tr}(N_{tr} + 1). \end{aligned} \quad (33)$$

These expressions for $I_{2,3}$ contain both non-universal terms (as is evident from the dependency on N_{tr}) and potential universal terms. The question becomes how to identify which is which. We do so by comparison with the evaluation of I_2 and I_3 in Refs. [43, 44] already given in Eqn.(29). At $x = 2$, $I_2(x = 0)$ is purely non-universal, i.e. $I_{2,univ.}(x = 2) = 0$.

This corresponds to our finding that I_2 is proportional to $N_{tr}(N_{tr} + 1)$ and indicates that the regulator, ϵ_p , used in Ref. [43, 44] can be identified with the TCSA regulator via $\epsilon_p^{-2} \propto N_{tr}(N_{tr} + 1)$. However I_3^{TCSA} is also proportional to $N_{tr}(N_{tr} + 1)$, which seems to imply that the third order contribution to E_{gs} , as with second order, is purely non-universal. We see then already at $x = 2$ that the TCSA regulator leads to a different universal structure to $E_{0,univ}$ than the Lorentz invariant regulator employed in [43, 44].

We verify the accuracy of this perturbative computation by comparing it with the TCSA numerics. In Fig.5 we plot E_0 at small g evaluated numerically against the perturbative results. We obtain excellent agreement. To analyze more closely the possible presence of a universal term in the numerics, we plot in Fig. 6 the residual ground state energy arrived at by subtracting from the numerical data the perturbative contributions (solely non-universal) corresponding to $I_2^{TCSA} + I_3^{TCSA}$. To determine whether the numerics indicate any universal contribution, we plot the residual as a function of g and fit the results to a function of the form $g^3(a + gbN_{tr}(N_{tr} + 1))$. These fits put an approximate bound (the value of a) on the third order universal term consistent with the numerics. We find it to be considerably smaller than that found in Ref. [43, 44], consistent with our previous statement that in the regulation scheme used by the TCSA, there is no universal term at third order in the coupling.

To get at the origin of the discrepancy between the TCSA evaluation of $E_{0,univ}$ and that of Refs. [43, 44], we evaluate the integrals, I_2 and I_3 in the TCSA regulation scheme away from the marginal point. These integrals have the structure (compare with Eqn. 28)

$$\begin{aligned}
I_2^{TCSA}(x, N_{tr}) &= I_{2,div.}^{TCSA}(x)(N_{tr}(N_{tr} + x - 1))^{x-1} + I_{2,univ.}^{TCSA}(x) + I_{2,subleading}^{TCSA}N_{tr}^{2x-6}; \\
I_3^{TCSA}(x, N_{tr}) &= I_{3,div.}^{TCSA}(x)(N_{tr}(N_{tr} + x - 1))^{x-1} + I_{3,univ.}^{TCSA}(x) + I_{3,subleading}^{TCSA}N_{tr}^{2x-4}. \quad (34)
\end{aligned}$$

We can evaluate the divergent and universal parts exactly (see Appendices A.4 and A.5)

$$\begin{aligned}
I_{2,div.}^{TCSA}(x) &= \frac{2\pi}{\Gamma^2(x)(2x - 2)}; \\
I_{2,univ.}^{TCSA}(x) &= \frac{\pi\Gamma^2(\frac{x}{2})\Gamma(1 - x)}{\Gamma^2(1 - \frac{x}{2})\Gamma(x)}; \\
I_{3,div.}^{TCSA}(x) &= \frac{12\pi^2}{\Gamma(\frac{x}{2})^6} \int_0^1 dj \int_0^j d\bar{j} \int_0^{1-j} dl \int_0^{1-j} dk \frac{(j\bar{j}kl(l + j - \bar{j})(k + j - \bar{j}))^{\frac{x}{2}-1}}{(j + l)(k + j)};
\end{aligned}$$

$$\begin{aligned}
I_{3,univ.}^{TCSA}(x) &= -\frac{2-x}{4-3x} \frac{1}{2} (L_{11}L_{12} + L_{21}L_{22}); \\
L_{11} &= \frac{\sqrt{\pi}}{2^x \sin(\frac{\pi x}{2})} \frac{\Gamma(1-\frac{x}{2})\Gamma(1-\frac{3x}{4})\Gamma(\frac{3}{2}-\frac{x}{2})\Gamma(\frac{x}{4})\Gamma(\frac{x}{2})}{\Gamma(\frac{x}{2})\Gamma(2-x)\Gamma^2(1-\frac{x}{4})}; \\
L_{12} &= -\frac{\pi(x-2)B(\frac{x}{2}, \frac{x}{2})}{2 \sin(\frac{\pi x}{2})} {}_3F_2(2-\frac{x}{2}, \frac{x}{2}, \frac{x}{2}, 2, x, 1); \\
L_{21} &= L_{11}; \\
L_{22} &= B(\frac{x}{2}, \frac{x}{2}-1)\Gamma(\frac{x}{2})\Gamma(1-\frac{x}{2}) {}_3F_2(\frac{x}{2}, \frac{x}{2}-1, 1-\frac{x}{2}, x-1, 1, 1), \tag{35}
\end{aligned}$$

where $B(x, y)$ is the β -function and ${}_3F_2$ is a generalized hypergeometric function. The subleading terms we are only able to evaluate numerically. Close to $x = 2$ we find

$$\begin{aligned}
I_{2,subleading}^{TCSA}(x=2) &= 0; \\
I_{3,subleading}^{TCSA}(x=2) &= 2\pi^2. \tag{36}
\end{aligned}$$

Plots of their values near $x = 2$ can be found in Appendices A.4 and A.5.

Now how does this compare to the results of [43, 44]? Remarkably the universal (constant) parts of I_2 and I_3 are the same (compare Eqn. (28)):

$$\begin{aligned}
I_{2,univ.}^{TCSA}(x) &= I_{2,univ.}(x); \\
I_{3,univ.}^{TCSA}(x) &= I_{3,univ.}(x). \tag{37}
\end{aligned}$$

In particular

$$\begin{aligned}
I_{2,univ.}^{TCSA}(x \sim 2) &= -\frac{\pi}{4}(2-x); \\
I_{3,univ.}^{TCSA}(x \sim 2) &= -2\pi^2. \tag{38}
\end{aligned}$$

We however see discrepancies in the subleading term, $I_{3,subleading}$:

$$I_{3,subleading}(x \sim 2) = \frac{3\pi^2}{2}; \quad I_{3,subleading}^{TCSA}(x \sim 2) = 2\pi^2. \tag{39}$$

This difference is a consequence of the TCSA's different (non-Lorentz invariant) regulator. It is possible to understand this difference as $I_{3,subleading}$ is finite at $x = 2$ due to a cancellation in a pole term due to an OPE and a zero in $I_{2,univ}$. This delicate cancellation leaves $I_{3,subleading}$ sensitive to choice of regulator in a way that $I_{3,univ}$ is not.

What are then the implications of $I_{3,subleading}(x)$ depending upon the regulator? Firstly we obtain an altered Zamolodchikov c-function:

$$c_{TCSA}(\tilde{g}(l)) = c + 24\pi \left(-\frac{3\pi(2-x)}{4} \frac{\tilde{g}^2(l)}{8} - \tilde{g}^3(l) \left(\frac{b\pi^2}{12} (1 - \epsilon_{TCSA}^{2-x}) \right) \right) \quad (40)$$

where $\epsilon_{TCSA} = N_{tr}^{-1}$. Interestingly the TCSA c-function agrees with that derived previously in Ref. [44] for $x < 2$ in the large N_{tr} (small ϵ_p) limit. However it is not solely a function of $\tilde{g}(l)$ as would be suggested by scaling theory.

As we have already noted, at $x = 2$ the $\tilde{g}^3(l)$ term vanishes in $c_{TCSA}(\tilde{g})$. This suggests that corrections that contribute to the universal part of the ground state energy are sensitive to the use of a non-Lorentz invariant regulator. It is interesting to note that these Lorentz invariant corrections are seen in models which are the *lattice* equivalent of these field theories and so do not have Lorentz invariance. Ref. [50], using a quantum transfer matrix approach, has analyzed the XXX Heisenberg model, a lattice equivalent of $SU(2)_1$ with a marginally irrelevant current-current interaction. In this work it is shown that the g^3 term as computed in Refs. [44, 51] using a Lorentz-invariant regulator is seen in the low temperature specific heat of the spin chain. At least for the XXX spin chain, terms in its field theoretic equivalent Hamiltonian that break Lorentz invariance are irrelevant rather than marginal in nature [51].

An interesting possibility [52] is that the universal structure of the ground state energy as determined in a Lorentz invariant field theory remains in the presence of a non-Lorentz invariant regulator provided one allows the ‘‘speed of light’’ in the system to be renormalized by the interactions (a possibility if Lorentz invariance is broken), that is to say that all of the consequences of breaking Lorentz invariance reside in a renormalization of c . Because the ground state energy depends upon $1/c$ (throughout this paper we have set the bare value of c to 1), we cannot distinguish between a breaking of universality in the ground state energy and a renormalization of c .

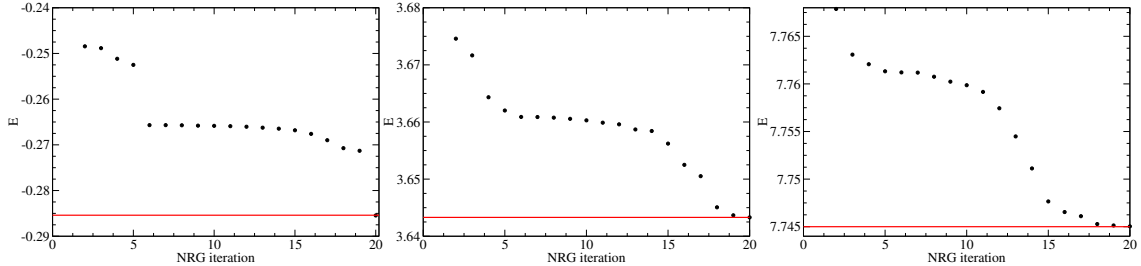


FIG. 7: Plots of the ground state (left), the first excited state (center), and the fifth excited state (right) energies as a function of RG step. The energies of the last RG step correspond to taking into account all states up to a truncation of $N_{tr} = 11$. Here $g = 0.008$ is marginally irrelevant. The NRG base matrix size and step size (N and Δ in the notation of [22]) are $N = 4767$ and $\Delta = 500$. The total number of states in the Verma module of the Identity is 14767. The solid line is the TCSA result done with an exact diagonalization at level $N_{tr} = 11$.

B. NRG and Marginal Perturbations

In this subsection we apply the numerical renormalization group to the study of the marginal current-current perturbation of $SU(2)_1$. The NRG is a technique that allows the TCSA to include states at much higher conformal levels than would be possible with a straight exact diagonalization. It does so by taking a cue from Kenneth Wilson’s NRG [47]: it takes into account the states that have a weaker influence on the low energy eigenstates of the full theory, in this case high energy conformal states, only in numerically manageable chunks. It works in the case of a relevant perturbation because such perturbations guarantee that the high energy conformal Hilbert space only affects weakly the low energy sector of the theory. Thus it is not clear, *a priori*, whether the NRG will work in the case of a marginal perturbation where the high and low energy sectors of the theory are more tightly coupled. We will, however, see that the NRG does work, reproducing with high accuracy the results of the TCSA run with a straight exact diagonalization.

Fig. 7 shows the RG evolution of the energies of the ground state, the first excited state, and the fifth excited state. The NRG results converge towards the exact diagonalization results with excellent accuracy. At least for the low lying energies in marginally perturbed conformal field theories, the NRG seems to be able to reproduce the expected energies, despite their dependencies upon the TCSA UV cutoff, N_{tr} .

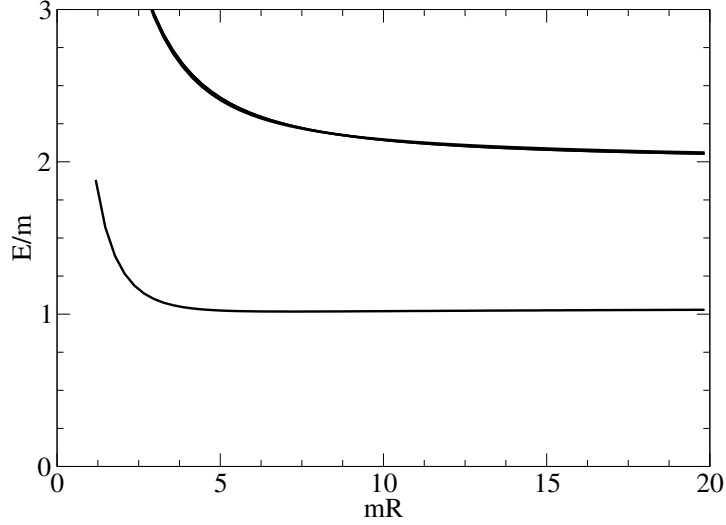


FIG. 8: Plot of the energies of the four lowest excited states as a function of R in the sector $S_z = 0$. The ground state energy has been subtracted. The data are found for a truncation level $N_{tr} = 6$. There is a single low lying state with mass $M = 1.001$ and spin $S_z = 0$, which is a member of the fundamental triplet of particles. The higher energy level is three fold degenerate and corresponds to two-particle states.

V. $SU(2)_2$ PERTURBED BY THE SPIN-1 FIELD

In this section we apply the TCSA to a deformation of the $SU(2)_2$ WZW model [2]. The $SU(2)_2$ WZW model is a $c = \frac{3}{2}$ conformal field theory with three primary fields, the spin-0 identity field, a spin $\frac{1}{2}$ field, $\phi_{1/2, \pm 1/2}$, and a spin 1 field, $\phi_{1, \{\pm 1, 0\}}$, with conformal weights $\Delta = 0$, $\Delta_{1/2} = \frac{3}{16}$, and $\Delta_1 = \frac{1}{2}$ respectively.

$SU(2)_2$ WZW can be thought of as a theory of three non-interacting massless Majorana fermions (the spin-1 fields). Perturbing $SU(2)_2$ with the spin-1 field,

$$H = H_{SU(2)_2} + g \int dx (\phi_{1,1} \bar{\phi}_{1,-1} - \phi_{1,0} \bar{\phi}_{1,0} + \phi_{1,-1} \bar{\phi}_{1,1}), \quad (41)$$

makes the fermions massive. Finding such a spectrum however is a strong check on the TCSA as the massive Majorana fermions are not simply expressible in the conformal current algebra basis.

Fig. 8 shows the low lying excited states from the TCSA. The coupling g is fixed to a value where the mass of the first excited state is 1. The TCSA captures this state (the $S_z = 0$ state of the triplet of massive Majoranas) as well as a set of three two particle states

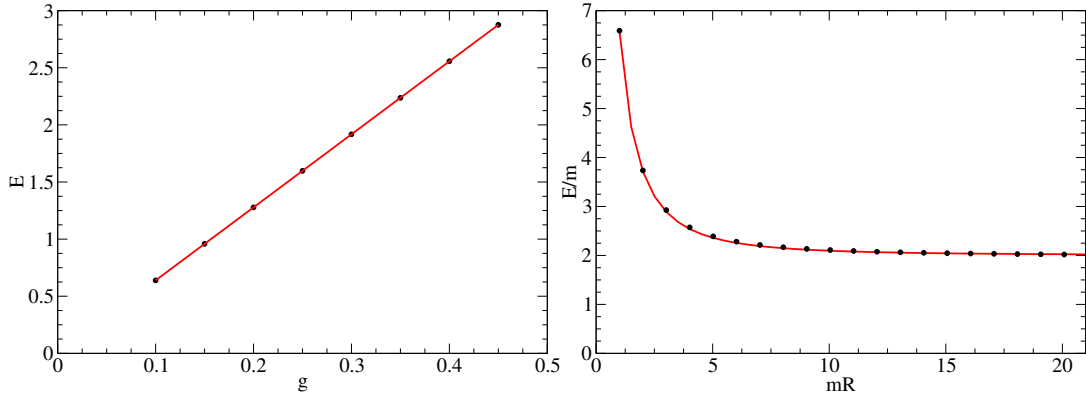


FIG. 9: a) Linear scaling of the mass of the triplet with the coupling g . b) A comparison of the energy of a two-particle state with $(n_1, n_2) = (-1, 1)$ between TCSA numerics (black dots) and analytics (solid red line).

with an energy approximately equal to 2. The Majorana fermions are non-interacting, hence their mass must scale linearly with g . This behavior is shown in Fig. 9a. We also consider the finite size corrections to one of the two-particle states. Even though non-interacting, the quantization condition for the two-particle state, Eqn. 21, is non-trivial as one needs to quantize with a doublet of distinct integers (n_1, n_2) , $n_1 \neq n_2$. Fig. 9b shows that the TCSA energy of the two-particle state matches the prediction derived from Eqn. 21.

VI. CONCLUSIONS AND DISCUSSIONS

In this paper we have applied the TCSA to perturbations of $SU(2)_k$. The general methodology is illustrated with various examples. We began by studying the $SU(2)_1 + Tr(g)$ perturbation, equivalent to the sine-Gordon model at a particular value of its coupling. We showed the TCSA accurately captured both the ground state energy and excited state spectrum including finite size corrections. We next turned to $SU(2)_1 + \bar{J}_L \cdot \bar{J}_R$, a WZW model perturbed by a marginal interaction. We demonstrated that one can accurately identify analytically the leading UV divergences in perturbation theory that characterize the ground state energy as computed numerically by the TCSA. By subtracting these UV divergences (i.e. the non-universal contributions to the ground state energy) we isolated the universal contribution to the ground state energy due to the marginal perturbation. We find that it differs from that predicted with calculations using Lorentz invariant regulators. Inter-

estingly, away from the marginal point, the universal structure of the ground state energy is restored. Finally we considered $SU(2)_2$ perturbed by $Tr(g)^2$. This model is equivalent to three massive non-interacting Majorana fermions. The TCSA, is able to reproduce the expected spectrum. This is a non-trivial check of our methodology as the Majorana fermions do not have a simple representation in the current algebra basis employed by the approach.

We have developed this capability to study perturbed WZW models in order to tackle a number of problems. In particular, we have two in mind. In the first, we plan to examine the dimerized-frustrated $J_1 - J_2 - \delta$ Heisenberg model whose Hamiltonian is

$$H = \sum_n J_1 (1 + \delta(-1)^n) \bar{S}_n \cdot \bar{S}_{n+1} + J_2 \bar{S}_n \bar{S}_{n+2}. \quad (42)$$

Field theory analyses [27] argue that the low energy sector of this theory is equivalent to

$$H = H_{SU(2)_1} + g \int dx \bar{J}_R \cdot \bar{J}_L + h \int dx (\phi_{1/2,1/2} \bar{\phi}_{1/2,-1/2} - \phi_{1/2,-1/2} \bar{\phi}_{1/2,1/2}), \quad (43)$$

where $g \propto J_2 - J_{2c}$ and $h \propto \delta$. If the marginal perturbation g is absent, the model's spin gap, Δ_S , would scale simply with h : $\Delta_S \propto h^{2/3}$. In the presence of g , however, this scaling is altered to become $\Delta_S \propto h^{2/3}/|\log(h)|^{1/2}$. However this altered scaling has been difficult to see in DMRG studies of the dimerized-frustrated Heisenberg model [28, 29]. It would be extremely interesting to analyze this scaling behavior using the TCSA.

Our study here of $SU(2)_1 + \bar{J}_L \cdot \bar{J}_R$ has thus laid the groundwork for this future study.

The second problem that we intend to tackle is the study of possible integrable perturbations of $SU(2)_k$ for $k > 1$. There are indications, coming from Zamolodchikov-type counting arguments [48], that those perturbations do exist. We intend to study these perturbations with the TCSA, extracting both the spectrum of the model as well as evidence for or against their integrability. The example analyzed in this paper concerning $SU(2)_2$ shows that this goal is within reach.

Acknowledgments

We thank J. Cardy, F. H. L. Essler, G. Mussardo and G. Takacs for useful discussions. L.L. acknowledges a grant awarded by Banco de Santander and financial support from European Regional Development Fund. R.M.K. acknowledges support by the US DOE under contract

DE-AC02-98CH10886 and NSF under grant no. PHY 1208521. G.S. acknowledges support from the grants FIS2009-11654, QUITEMAD and the Severo-Ochoa Program. G.P.B. acknowledges support from the Netherlands Organisation for Scientific Research (NWO).

Appendix A: Evaluation of the Perturbative Integrals from the Current-Current Perturbation of $SU(2)_1$

1. TCSA regularization and the Lehmann representation

We implement the UV regularization explicit in the TCSA with a truncation of the Lehmann representation of the n -point functions [46, 49]. As an explicit example, we compute the two point function using this truncation. Introducing projectors $\mathcal{P}_{N_{tr}}$ and $\bar{\mathcal{P}}_{N_{tr}}$ that project out all chiral states of level higher than N_{tr} , we can write the two point function appearing in the evaluation of the second order perturbative contribution to the ground state energy as

$$\langle \mathcal{T} \phi(x, t) \phi(0, 0) \rangle = \langle \mathcal{T} \mathcal{P}_{N_{tr}} \bar{\mathcal{P}}_{N_{tr}} \phi(x, t) \mathcal{P}_{N_{tr}} \bar{\mathcal{P}}_{N_{tr}} \phi(0, 0) \mathcal{P}_{N_{tr}} \bar{\mathcal{P}}_{N_{tr}} \rangle, \quad (\text{A1})$$

where \mathcal{T} is the usual time ordering operator. These projectors act to truncate the Lehmann mode expansion arising from the insertion of the resolution of the identity in between the fields of (A1):

$$\sum_{0 \leq m, \bar{m} \leq N_{tr}} \langle 0 | \phi(0, 0) | m \rangle \otimes | \bar{m} \rangle \langle m | \otimes \langle \bar{m} | \phi(x, t) | 0 \rangle. \quad (\text{A2})$$

Here the truncated sum is over all states whose conformal level is less than N_{tr} and we just considered the contribution with $t < 0$. Using the time and space translation operator, $e^{-Ht - iPx}$, and defining $z = e^{\frac{2\pi}{R}(ix+t)}$ and $\bar{z} = e^{\frac{2\pi}{R}(-ix+t)}$, we can rewrite the above as

$$\sum_{0 \leq m, \bar{m} \leq N_{tr}} \langle 0 | \phi(0, 0) (|m\rangle \otimes |\bar{m}\rangle \langle m| \otimes \langle \bar{m}|) \phi(0, 0) | 0 \rangle z^m \bar{z}^{\bar{m}}, \quad (\text{A3})$$

so reducing the correlation function to a sum over powers in z and \bar{z} . We see in this sum that no power greater than N_{tr} of z or \bar{z} appears.

The case of the third order correction to the energy involving a three-point function follows the same strategy. We insert the projectors

$$\langle \mathcal{T} \mathcal{P}_{N_{tr}} \bar{\mathcal{P}}_{N_{tr}} \phi(x, t) \mathcal{P}_{N_{tr}} \bar{\mathcal{P}}_{N_{tr}} \phi(0, 0) \mathcal{P}_{N_{tr}} \bar{\mathcal{P}}_{N_{tr}} \phi(x', t') \mathcal{P}_{N_{tr}} \bar{\mathcal{P}}_{N_{tr}} \rangle, \quad (\text{A4})$$

arriving, in the case where $t' < 0 < t$, at

$$\sum_{0 \leq m, \bar{m}, n, \bar{n} \leq N_{tr}} \langle 0 | \phi(x, t) | m \rangle \otimes | \bar{m} \rangle \langle m | \otimes \langle \bar{m} | \phi(0, 0) | n \rangle \otimes | \bar{n} \rangle \langle n | \otimes \langle \bar{n} | \phi(x', t') | 0 \rangle. \quad (\text{A5})$$

If we again use the space time translation operator and use the notation $z = e^{\frac{2\pi}{R}(ix+t)}$, $\bar{z} = e^{\frac{2\pi}{R}(-ix+t)}$, $w = e^{\frac{2\pi}{R}(ix'+t')}$, and $\bar{w} = e^{\frac{2\pi}{R}(-ix'+t')}$, we obtain

$$\sum_{0 \leq m, \bar{m}, n, \bar{n} \leq N_{tr}} \langle 0 | \phi(0, 0) | m \rangle \otimes | \bar{m} \rangle \langle m | \otimes \langle \bar{m} | \phi(0, 0) | n \rangle \otimes | \bar{n} \rangle \langle n | \otimes \langle \bar{n} | \phi(0, 0) | 0 \rangle z^{-m} \bar{z}^{-\bar{m}} w^n \bar{w}^{\bar{n}}, \quad (\text{A6})$$

that is a truncated polynomial at order N_{tr} in z, \bar{z}, w, \bar{w} .

2. Evaluation of I_2 at $x = 2$

We want to compute the integral, I_2^{TCSA} , by regularizing as we did with (A1). Transforming the integral in I_2 back to the cylinder we obtain,

$$I_2^{TCSA} = 2 \cdot \left(\frac{2\pi}{R} \right)^2 \int_0^R dx \int_{-\infty}^0 dt \frac{z}{(z-1)^2} \frac{\bar{z}}{(\bar{z}-1)^2}, \quad (\text{A7})$$

where the factor of two counts the two contributions coming from time ordering. If we then expand the integrand as a power series in z, \bar{z} and compare with Eqn. A3, we see we should truncate the sum as follows

$$I_2 = 2 \cdot \left(\frac{2\pi}{R} \right)^2 \int_0^R dx \int_{-\infty}^0 dt \sum_{n=0}^{N_{tr}} n z^n \sum_{\bar{n}=0}^{N_{tr}} \bar{n} \bar{z}^{\bar{n}}, \quad (\text{A8})$$

whereupon the integral and sum are easily computed:

$$I_2 = \pi N_{tr} (N_{tr} + 1). \quad (\text{A9})$$

Comparing with the evaluation in [43, 44], we see that we obtain a relationship between the TCSA regulator and the short distance cutoff, ϵ_p , used in [43, 44]:

$$\epsilon_p = \frac{1}{\sqrt{N_{tr}(N_{tr} + 1)}}. \quad (\text{A10})$$

3. Evaluation of I_3 at $x = 2$

We now turn to computing I_3^{TCSA} :

$$I_3^{TCSA} = \int dz d\bar{z} dw d\bar{w} \frac{1}{(z-w)(\bar{z}-\bar{w})(z-1)(w-1)(\bar{z}-1)(\bar{w}-1)}. \quad (\text{A11})$$

Moving to the cylinder, the time ordering gives 6 contributions, $t < t' < 0$, $t > t' > 0$, $t < 0 < t'$ and those with $t \leftrightarrow t'$, all being equal. We show, as an example, the integral for $t > 0 > t'$:

$$\left(\frac{2\pi}{R}\right)^4 \int_0^R dx \int_0^R dx' \int_0^\infty dt \int_{-\infty}^0 dt' \frac{z \bar{z} w \bar{w}}{(z-w)(\bar{z}-\bar{w})(z-1)(w-1)(\bar{z}-1)(\bar{w}-1)}, \quad (\text{A12})$$

where $z = e^{\frac{2\pi}{R}(ix+t)}$, $\bar{z} = e^{\frac{2\pi}{R}(-ix+t)}$, $w = e^{\frac{2\pi}{R}(ix'+t')}$, and $\bar{w} = e^{\frac{2\pi}{R}(-ix'+t')}$. We compute the contribution this makes by expanding the above in a power series of z, \bar{z}, w, \bar{w} and truncating it at the N_{tr} -th power, matching the truncation in the Lehmann expansion in Eqn. A6. The integrand in (A12) then becomes

$$\frac{|z|^2 |w|^2}{|z-w|^2 |z-1|^2 |w-1|^2} = \frac{1}{|1-w/z|^2} \frac{1}{|1-1/z|^2} \frac{1}{|1-w|^2} \frac{|w|^2}{|z|^2} \quad (\text{A13})$$

$$\begin{aligned} &= \sum_{j,k,\bar{j},\bar{k},\bar{l} \in C} \left(\frac{z}{w}\right)^{j+1} \left(\frac{\bar{z}}{\bar{w}}\right)^{\bar{j}+1} z^{-k} \bar{z}^{-\bar{k}} w^l \bar{w}^{\bar{l}} \\ &= \sum_{j,k,\bar{j},\bar{k},\bar{l} \in C} w^{j+l+1} \bar{w}^{\bar{j}+\bar{l}+1} z^{-k-j-1} \bar{z}^{-\bar{k}-\bar{j}-1}, \end{aligned} \quad (\text{A14})$$

where C is defined by

$$\begin{aligned} 1 &\leq j+l+1 \leq N_{tr}; \\ 1 &\leq j+k+1 \leq N_{tr}; \\ 1 &\leq \bar{j}+\bar{l}+1 \leq N_{tr}; \\ 1 &\leq \bar{j}+\bar{k}+1 \leq N_{tr}. \end{aligned} \quad (\text{A15})$$

and all the indexes are positive or zero. The integrals can now be done and the sum that so arises evaluated to be

$$\pi^2 \sum_C \frac{1}{(j+l+1)(j+k+1)} = \pi^2 \frac{N_{tr}(N_{tr}+1)}{2}. \quad (\text{A16})$$

Once combined with the other five equal contributions, we obtain the final result:

$$I_3^{TCSA} = 3\pi^2 N_{tr}(N_{tr}+1). \quad (\text{A17})$$

4. Evaluation of $I_2^{TCSA}(x)$

For general x , I_2 once transformed back onto the cylinder reads

$$I_2^{TCSA}(x) = 2 \cdot \left(\frac{2\pi}{R}\right)^2 \int_0^R dx \int_{-\infty}^0 dt \frac{|z|^x}{|z-1|^{2x}}. \quad (\text{A18})$$

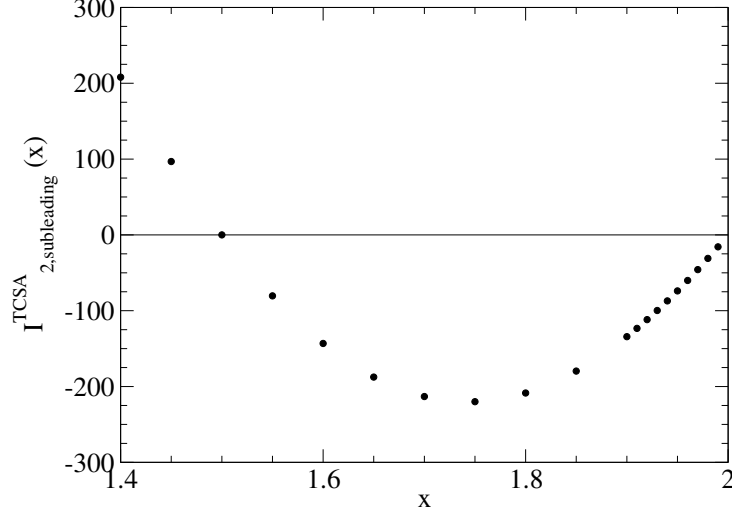


FIG. 10: Plot of $I_{2,subleading}^{TCSA}(x)$ as a function of x .

Expanding the integrands in powers of z and \bar{z} , truncating with level N_{tr} , and performing the integrals leaves us with (compare Eqn. (A8))

$$\begin{aligned}
I_2^{TCSA}(x) &= 2\pi \sum_{n=0}^{N_{tr}-1} \frac{\Gamma^2(n+x)}{(n+\frac{x}{2})\Gamma^2(x)(n!)^2} \\
&\equiv I_{2,div.}^{TCSA}(x)(N_{tr}(N_{tr}+x-1))^{x-1} + I_{2,univ.}^{TCSA}(x) + I_{2,subleading}^{TCSA}(x)N_{tr}^{2x-6}. \quad (A19)
\end{aligned}$$

The coefficient of the first term in the above can be determined from the Euler-Maclaurin formula converting a sum to an integral in combination with our exact result at $x=2$. The result is

$$I_{2,div.}^{TCSA}(x) = \frac{2\pi}{\Gamma^2(x)(2x-2)}. \quad (A20)$$

The universal term, $I_{2,univ.}^{TCSA}$, can be determined from performing the integral in Eqn. (A18) for $0 < x < 1$ and then analytically continuing [43]:

$$I_{2,univ.}^{TCSA}(x) = \frac{\pi\Gamma^2(\frac{x}{2})\Gamma(1-x)}{\Gamma^2(1-\frac{x}{2})\Gamma(x)}. \quad (A21)$$

Finally we determine $I_{2,subleading}^{TCSA}(x)$ numerically: we compute the sum in Eqn. (A19) numerically as a function of N_{tr} , subtract the first two terms in the second line of Eqn. (A19), and fit the remainder to extract the coefficient of N_{tr}^{2x-6} . The results are plotted in Fig. (10). We note in particular that as $x \rightarrow 2$, $I_{2,subleading}^{TCSA}(x) \rightarrow 0$.

5. Evaluation of $I_3^{TCSA}(x)$

$I_3^{TCSA}(x)$ is computed by first reexpressing $I_3(x)$ as an integral over the cylinder:

$$I_3(x) = \left(\frac{2\pi}{4}\right)^4 \int_0^R dx_1 dx_2 \int_{-\infty}^{\infty} dt_1 dt_2 \frac{|z_1|^x |z_2|^x}{|z_1 - z_2|^x |z_1 - 1|^x |z_2 - 1|^x}, \quad (\text{A22})$$

where $z_i = e^{2\pi(ix_i + t_i)/R}$. Expanding the integrand in powers of z_i and truncating these sums on the basis of a comparison with the Lehmann expansion leaves us with

$$I_3^{TCSA}(x) = 12\pi^2 \sum_{j=0}^{N_{tr}-1} \sum_{\bar{j}=0}^{N_{tr}-1} \sum_{j=0}^j \sum_{l=0}^{N_{tr}-j-1} \sum_{k=0}^{N_{tr}-j-1} \frac{\gamma_j \gamma_{\bar{j}} \gamma_l \gamma_{j+l-\bar{j}} \gamma_k \gamma_{k+j-\bar{j}}}{(j+l+\frac{x}{2})(j+k+\frac{x}{2})};$$

$$\gamma_j = \frac{\Gamma(j+\frac{x}{2})}{\Gamma(\frac{x}{2})\Gamma(j+1)}. \quad (\text{A23})$$

$I_3^{TCSA}(x)$ then has a similar structure to $I_2^{TCSA}(x)$:

$$I_3^{TCSA}(x) = I_{3,div.}^{TCSA}(x)(N_{tr}(N_{tr}+x-1))^{x-1} + I_{3,univ.}^{TCSA}(x) + I_{3,subleading}^{TCSA}(x)N_{tr}^{x-2}. \quad (\text{A24})$$

We infer that the leading term of $I_3^{TCSA}(x)$ must be proportional to $(N_{tr}(N_{tr}+x-1))^{x-1}$ – otherwise the relationship between the TCSA cutoff, N_{tr} , and ϵ_p established in the evaluation of I_2 would breakdown. (We will in any case verify this numerically in what is to come.)

The coefficient of the leading term can be found by converting the sums to integrals:

$$I_{3,div.}^{TCSA}(x) = \frac{12\pi^2}{\Gamma^6(\frac{x}{2})} \int_0^1 dj \int_0^j d\bar{j} \int_0^{1-j} dl \int_0^{1-j} dk \frac{(j\bar{j}lk(l+j-\bar{j})(k+j-\bar{j}))^{\frac{x}{2}-1}}{(j+l)(k+l)}. \quad (\text{A25})$$

We can also evaluate analytically $I_{3,univ.}^{TCSA}(x)$. This can be computed by performing the integral in Eqn. (24) for values of x where it is convergent and then analytically continuing. To make this evaluation we first perform the integration by parts suggested in Ref. [44]:

$$I_{3,univ.}^{TCSA}(x) = I_{3,univ.}(x) = \frac{2-x}{4-3x} \int d^2 z_1 d^2 z_2 \frac{|z_1+1|^{x-2} |z_2+1|^{x-2}}{|z_1-z_2|^x |z_1|^x |z_2|^x} \left(\frac{z_1}{1+z_1} + \frac{\bar{z}_1}{1+\bar{z}_1} \right). \quad (\text{A26})$$

We now evaluate this integral following the techniques introduced in Ref. [53] and used in Ref. [54]. Writing $z_i = x_i + iy_i$ and making the changes of variables:

$$y_i \rightarrow ie^{-i2\epsilon} y_i, \quad (\text{A27})$$

followed by

$$y_{\pm} = x_1 \pm y_1; \quad w_{\pm} = x_2 \pm y_2, \quad (\text{A28})$$

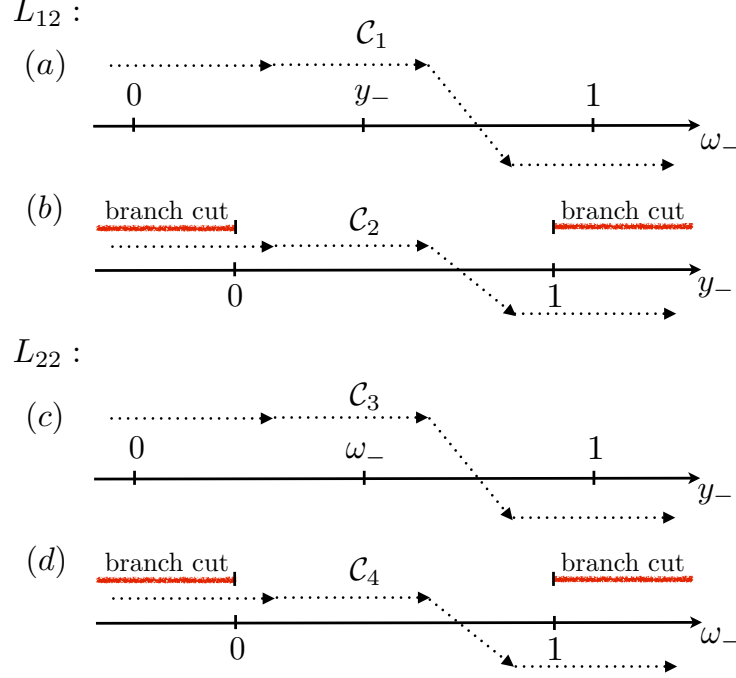


FIG. 11: Definition of contours used in evaluating $I_{3,univ}^{TCSA}(x)$. There are branch points at all labelled points: $0, 1, y_-,$ and w_- . The red lines mark additional branch cuts with branch points at 0 and 1 that result from integrating w_- in the case of L_{12} and y_- in the case of L_{22} .

allows us to rewrite $I_3(x)$ as

$$\begin{aligned}
I_3(x) &= \frac{2-x}{2(4-3x)} \int dy_+ (y_+ - 1 - i\epsilon\Delta_y)^{\frac{x}{2}-1} (y_+ - i\epsilon\Delta_y)^{-\frac{x}{2}} \\
&\times \int dw_+ (w_+ - y_+ - i\epsilon(\Delta_w - \Delta_y))^{-\frac{x}{2}} (w_+ - 1 - i\epsilon\Delta_w)^{\frac{x}{2}-1} (w_+ - i\epsilon\Delta_w)^{-\frac{x}{2}} \\
&\times \int dy_- (y_- - 1 + i\epsilon\Delta_y)^{\frac{x}{2}-2} (y_- + i\epsilon\Delta_y)^{-\frac{x}{2}+1} \\
&\times \int dw_- (w_- - y_- + i\epsilon(\Delta_w - \Delta_y))^{-\frac{x}{2}} (w_- - 1 + i\epsilon\Delta_w)^{\frac{x}{2}-1} (w_- + i\epsilon\Delta_w)^{-\frac{x}{2}}, \quad (\text{A29})
\end{aligned}$$

where $\Delta_{w/y} = (w/y)_+ - (w/y)_-$. The positions of the contours for w_- and y_- relative to the various branch cuts of the arguments depend on the values of w_+ and y_+ . Only for certain values of w_+ and y_+ is it not possible to deform the contours w_-/y_- to infinity without encountering poles or branch cuts. This allows us to restrict the limits of w_+ and y_+ dramatically, simplifying the above integral to

$$I_3(x) = \frac{2-x}{2(4-3x)} (L_1 + L_2);$$

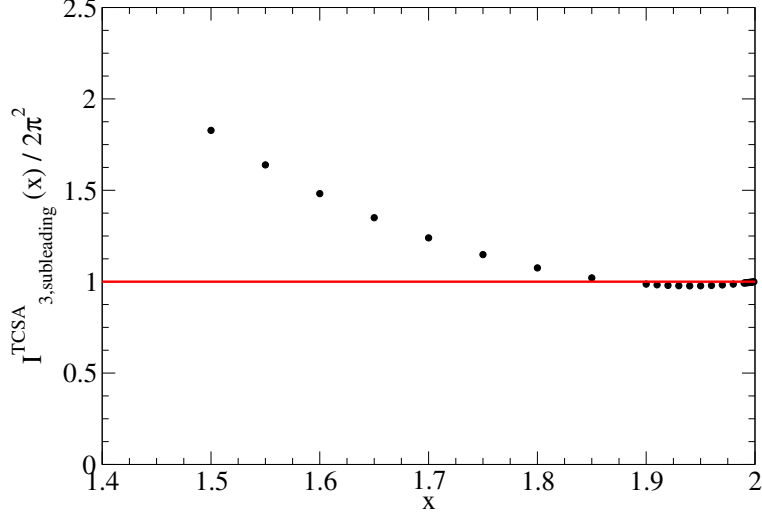


FIG. 12: Plot of $I_{3,subleading}^{TCSA}(x)/(2\pi)^2$ as a function of x .

$$L_1 = -L_{11}L_{12}; \quad L_2 = -L_{21}L_{22};$$

$$L_{11} = \int_0^1 dw_+ \int_0^{w_+} dy_+ (1-y_+)^{\frac{\alpha}{2}-1} w_+^{-\frac{\alpha}{2}} (w_+ - y_+)^{-\frac{\alpha}{2}} (1-w_+)^{\frac{\alpha}{2}-1} y_+^{-\frac{\alpha}{2}};$$

$$L_{12} = \int_{C_2} dy_- \int_{C_1} dw_- (1-y_-)^{\frac{\alpha}{2}-2} y_-^{-\frac{\alpha}{2}+1} (w_- - y_-)^{-\frac{\alpha}{2}} (1-w_-)^{\frac{\alpha}{2}-1} w_-^{-\frac{\alpha}{2}};$$

$$L_{21} = \int_0^1 dy_+ \int_0^{y_+} dw_+ (1-y_+)^{\frac{\alpha}{2}-1} w_+^{-\frac{\alpha}{2}} (y_+ - w_+)^{-\frac{\alpha}{2}} (1-w_+)^{\frac{\alpha}{2}-1} y_+^{-\frac{\alpha}{2}};$$

$$L_{22} = \int_{C_3} dy_- \int_{C_4} dw_- (1-y_-)^{\frac{\alpha}{2}-2} y_-^{-\frac{\alpha}{2}+1} (y_- - w_-)^{-\frac{\alpha}{2}} (1-w_-)^{\frac{\alpha}{2}-1} w_-^{-\frac{\alpha}{2}}. \quad (\text{A30})$$

The contours $C_i, i = 1, 2, 3, 4$ are defined in Fig. (11). These four separate integrals can now readily be expressed in terms of generalized hypergeometric functions with the results found in Eqn. (35).

Finally we can evaluate $I_{3,subleading}^{TCSA}(x)$ numerically. We compute this coefficient by evaluating the sum in Eqn. (A23) for a range of N_{tr} , subtracting off $I_{3,div}^{TCSA}$ and $I_{3,univ}^{TCSA}$. The remainder is proportional to N_{tr}^{x-2} and we extract $I_{3,subleading}^{TCSA}$ as the fitting coefficient. The

results are found in Fig. 12. We see in particular that $I_{3,subleading}^{TCSA}(x) \rightarrow 2\pi^2$ as $x \rightarrow 2$.

- [1] A. O. Gogolin, A. A. Nersesyan, and A. M. Tsvelik, *Bosonization and Strongly Correlated Systems*, Cambridge University Press, (1998); T. Giamarchi, *Quantum Physics in One Dimension*, Oxford University Press, (2004).
- [2] P. Di Francesco, P. Mathieu and D. Sénéchal, *Conformal field theory*, Springer (1997).
- [3] G. Mussardo, *Statistical Field Theory, An Introduction to Exactly Solved Models in Statistical Physics*, Oxford University Press, (2010).
- [4] M. Takahashi, *Thermodynamics of One-Dimensional Solvable Models*, Cambridge University Press (1999);
B. S. Shastry, S. S. Jha, V. Singh, *Exactly Solvable Problems in Condensed Matter and Relativistic Field Theory*, Lecture Notes in Physics, Springer-Verlag (1985).
- [5] V. P. Yurov and A. B. Zamolodchikov, Int. J. Mod. Phys. A **5** 3221 (1990).
- [6] S. R. White, Phys. Rev. Lett. **69** 2863 (1992); Phys. Rev. B **48**, 10345 (1993).
- [7] V. P. Yurov and A. B. Zamolodchikov, Int. J. Mod. Phys. A **6** 4557 (1991).
- [8] M. Lassig, G. Mussardo, and J. L. Cardy, Nucl. Phys. B **348** 591 (1991).
- [9] L. Lepori, G. Mussardo, and G. Z. Toth, J. Stat. Mech. **0809** P09004 (2008).
- [10] L. Lepori, G. Z. Toth, and G. Delfino, J. Stat. Mech. **0911** P11007 (2009).
- [11] G. Feverati, F. Ravanini and G. Takacs, Phys. Lett. B **430** 264 (1998).
- [12] G. Feverati, F. Ravanini and G. Takacs, Phys. Lett. B **444** 442 (1998).
- [13] Z. Bajnok, L. Palla, G. Takacs and F. Wagner, Nucl. Phys. B **601**, 503 (2001).
- [14] P. Dorey, I. Runkel, R. Tateo and G. M. T. Watts, Nucl. Phys. B **578** 85 (2000).
- [15] T. R. Klassen and E. Melzer, Nucl. Phys. B **370** 511 (1992).
- [16] P. Dorey and R. Tateo, Nucl. Phys. B **482** 639 (1996).
- [17] P. Dorey, A. J. Pocklington, R. Tateo and G. M. T. Watts, Nucl. Phys. B **525** 641 (1998).
- [18] T. R. Klassen and E. Melzer, Nucl. Phys. B **362**, 329 (1991).
- [19] G. Feverati, F. Ravanini and G. Takacs, Nucl. Phys. B **540** 543 (1999).
- [20] P. Fonseca and A. Zamolodchikov, J. Stat. Phys. **110** 527 (2003).
- [21] R. M. Konik and Y. Adamov, Phys. Rev. Lett. **98** 147205 (2007).
- [22] R. M. Konik and Y. Adamov, Phys. Rev. Lett. **102** 097203 (2009).

- [23] G. P. Brandino, R. M. Konik and G. Mussardo, J. Stat. Mech., P07013 (2010).
- [24] R. M. Konik, Phys. Rev. Lett. **106** 136805, (2011).
- [25] J.-S. Caux and R. M. Konik, Phys. Rev. Lett. **109** 175301 (2012).
- [26] I. Affleck and F. D. M. Haldane, Phys. Rev. B **36** 5291 (1987).
- [27] I. Affleck, D. Gepner, H. J. Schulz and T. Ziman, J. Phys. A **22** 511 (1989).
- [28] M. Kumar, S. Ramasesha, D. Sen and Z. G. Soos, Phys. Rev. B **75** 05204 (2007).
- [29] T. Barnes, J. Riera, and D. A. Tennant, Phys. Rev. B **59** 11384 (1999).
- [30] F.D.M. Haldane, Phys. Rev. Lett. **60** 635 (1988); B.S. Shastry, Phys. Rev. Lett. **60** 639 (1988).
- [31] J. I. Cirac and G. Sierra, Phys. Rev. B **81** 104431 (2010).
- [32] A. E. B. Nielsen, J. I. Cirac and G. Sierra, J. Stat. Mech. P11014 (2011).
- [33] R. Thomale, S. Rachel, P. Schmitteckert, and M. Greiter, Phys. Rev. B. **85**, 195149 (2012).
- [34] V.G. Knizhnik and A. B. Zamolodchikov, Nucl. Rev. B **247** 83 (1984).
- [35] I. Affleck, *Field Theory Methods and Quantum Critical Phenomena*, in *Fields, Strings and Critical Behavior*, Proc. Les Houches Summer School in Theoretical Physics (1988).
- [36] A. M. Tsvetlik, *Quantum Field Theory in Condensed Matter Physics*, 2nd edition, Cambridge University Press (2003).
- [37] Al. B. Zamolodchikov, Int. J. Mod. Phys. A**10** 1125 (1995).
- [38] A. B. Zamolodchikov and Al. B. Zamolodchikov, Nucl. Phys. B **379** 602 (1992).
- [39] Al. B. Zamolodchikov, Nucl. Phys. B **342** 695 (1990).
- [40] A. B. Zamolodchikov and Al. B. Zamolodchikov, Ann. Phys. **120** 253 (1979);
R. J. Baxter, *Exactly Solved Models in Statistical Mechanics*, Academic Press London (1982).
- [41] A. B. Zamolodchikov and Al. B. Zamolodchikov, Ann. Phys. **120** 253 (1979).
- [42] B. Berg, M. Karowski, P. Weisz and V. Kurak, Nucl. Phys. B **134** 253 (1979);
P. Wiegmann, Phys. Lett. B **142** 173 (1983).
- [43] J. L. Cardy, J. Phys. A. **19** L1093 (1986).
- [44] A. W. W. Ludwig and J. L. Cardy, Nucl. Phys. B **285** 687 (1987).
- [45] A. B. Zamolodchikov, JETP Lett. **43** 730 (1986).
- [46] G. M. T. Watts, Nucl. Phys. B **859**, 177 (2012); P. Giokas and G. M. T. Watts,
arXiv:1106.2448.
- [47] K. G. Wilson, Rev. Mod. Phys. **47** 773 (1975).
- [48] A.B. Zamolodchikov, Adv. Stud. Pure Math. **19**, 641 (1989).

- [49] G. Feverati, K. Graham, P. A. Pearce, G. Z. Toth and G. M. T. Watts, *J. Stat. Mech.* **0911** 03011 (2008).
- [50] A. Klümper and D. C. Johnston *Phys. Rev. Lett.* **84**, 4701 (2000).
- [51] S. Lukyanov, *Nucl. Phys. B* **522**, 533 (1998).
- [52] J. Cardy, private communication.
- [53] V. S. Dotsenko, *Nucl. Phys. B* **240** 687 (1989).
- [54] R. M. Konik and A. LeClair, *Nucl. Phys. B* **479** 619 (1996).